

Unusual Transformations of a Bipyridine Ligand in Attempts to Trap a Terminal Chromium(III) Alkylidene

Somying Leelasubcharoen, Kin-Chung Lam, Thomas E. Concolino, Arnold L. Rheingold, and Klaus H. Theopold*

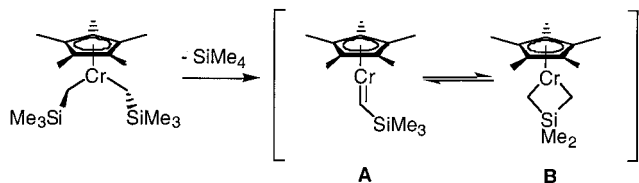
Department of Chemistry and Biochemistry, Center for Catalytic Science and Technology, University of Delaware, Newark, Delaware 19716

Received August 24, 2000

Attempts to trap a terminal chromium alkylidene by reactions of dialkyl $\text{Cp}^*\text{Cr}(\text{CH}_2\text{SiMe}_3)_2$ ($\text{Cp}^* = \eta^5\text{-C}_5\text{Me}_5$) or metallacycle $\text{Cp}^*(\text{THF})\text{Cr}(\text{CH}_2)_2\text{SiMe}_2$ with the bidentate ligand 1,2-bis(dimethylphosphino)ethane (dmpe) lead to dinuclear paramagnetic chromium alkyls $[\text{Cp}^*\text{Cr}(\text{CH}_2\text{SiMe}_3)_2]_2(\mu\text{-}\eta^1\text{:}\eta^1\text{-dmpe})$ (**1**) and $[\text{Cp}^*\text{Cr}(\text{CH}_2)_2\text{Si}(\text{CH}_3)_2]_2(\mu\text{-}\eta^1\text{:}\eta^1\text{-dmpe})$ (**2**), respectively. On the other hand, the unusual mononuclear chromium complex ($\eta^5\text{-pentamethylcyclopentadienyl})(2\text{'-}2\text{'-dimethyl-2\text{'-silapropyl})\text{-1,2-dihydro}[2,2\text{'}]$ bipyridine-1,3\text{'-diyl})-chromium(III) (**3**) was obtained by a reaction of $\text{Cp}^*(\text{THF})\text{Cr}(\text{CH}_2)_2\text{SiMe}_2$ with 1 equiv of 2,2'-bipyridine (bipy). **3** is formed by carbon–carbon bond formation between one terminus of the metallacycle and the 2-position of the bipy ligand, at the expense of the aromaticity of a pyridyl group. Single-electron oxidation of **3** with ferricenium hexafluorophosphate ($[\text{Cp}_2\text{-Fe}]\text{PF}_6$) yielded **4**, a dicationic dimer of **3** linked via a carbon–carbon bond between the bipy backbones. **1–4** were structurally characterized by X-ray diffraction.

Introduction

While chromium carbene complexes of the Fischer type mark the historical beginning of metal carbon multiple bonds and are abundant, simple alkylidenes of chromium remain rare. Recent examples include Gibson's spectroscopically characterized $(2,6\text{-}^i\text{Pr}_2\text{C}_6\text{H}_3\text{N})_2\text{(L)Cr}^{\text{VI}}=\text{CHCMe}_3$ ($\text{L} = \text{THF}, \text{PMe}_3$),¹ which surprisingly do not react with alkenes, and Scott's surface-grafted $(=\text{SiO})_2\text{Cr}^{\text{IV}}=\text{CHEMe}_3$ ($\text{E} = \text{C}, \text{Si}$), which initiate the polymerization of ethylene.^{2,3} Of particular interest in the context of our work on organometallics of trivalent chromium is Gambarotta's proposed $(\text{TMEDA})\text{Cr}^{\text{III}}\text{-(=CHPh)(CH}_2\text{Ph)}$.⁴ Over the years we have tried on occasion to isolate terminal $\text{Cp}^*\text{Cr}^{\text{III}}$ alkylidenes by various strategies, but to no avail. For example, neither deprotonation of cationic Cr^{III} alkyls⁵ nor steric crowding of Cr^{III} dialkyls yielded the desired species.⁶ While we have obtained several dinuclear complexes featuring bridging $\mu\text{-CHR}$ ligands ($\text{R} = \text{H}, \text{alkyl}$),^{7,8} a terminal Cr^{III} alkylidene has so far eluded us.



However, the various products of the thermal decomposition of the mononuclear 13-electron complex $\text{Cp}^*\text{Cr-}$

$(\text{CH}_2\text{SiMe}_3)_2$ have led us to propose a reaction mechanism in which an alkylidene (**A**) and a metallacyclobutane (**B**) intermediate coexist in rapid equilibrium.⁷ This raised the question whether the alkylidene might be trapped under suitable conditions. Specifically, since the structural chemistry of $\text{Cp}^*\text{Cr}^{\text{III}}$ is dominated by three-legged piano stools,⁹ the use of bidentate chelating ligands (L-L) might be expected to stabilize fragment **A** in the form of $\text{Cp}^*(\text{L-L})\text{Cr}=\text{CHSiMe}_3$. Herein we report on the dashing of that hope and on some remarkable chemistry accompanying yet another escape of the elusive Cr^{III} alkylidene.

Results and Discussion

Reaction of $\text{Cp}^*\text{Cr}(\text{CH}_2\text{SiMe}_3)_2$ with monodentate ligands merely produces adducts of the type $\text{Cp}^*(\text{L})\text{Cr-}(\text{CH}_2\text{SiMe}_3)_2$ ($\text{L} = \text{pyridine}, \text{THF}$). Following precedent from vanadium chemistry, where treatment of $\text{Cp}(\text{PMe}_3)\text{V}(\text{CH}_2\text{CMe}_3)_2$ with bis(dimethylphosphino)ethane (dmpe) yielded the alkylidene $\text{Cp}(\text{dmpe})\text{V}=\text{CHCMe}_3$,¹⁰ we reacted the chromium dialkyl with the same bidentate phosphine. However, treatment of orange $\text{Cp}^*\text{Cr-}(\text{CH}_2\text{SiMe}_3)_2$ with various amounts of dmpe yielded the dinuclear adduct $[\text{Cp}^*\text{Cr}(\text{CH}_2\text{SiMe}_3)_2]_2(\mu\text{-}\eta^1\text{:}\eta^1\text{-dmpe})$ (**1**, see Scheme 1).

* Corresponding author. E-mail: theopold@udel.edu.
 (1) Coles, M. P.; Gibson, V. C.; Clegg, W.; Elsegood, M. R. J.; Porrelli, P. A. *J. Chem. Soc., Chem. Commun.* **1996**, 1963.
 (2) Scott, S. L.; Ajjou, J. A. N.; Paquet, V. *J. Am. Chem. Soc.* **1998**, *120*, 415.
 (3) Ajjou, J. A. N.; Rice, G. L.; Scott, S. L. *J. Am. Chem. Soc.* **1998**, *120*, 13436.
 (4) Hao, S.; Song, J.-I.; Berno, P.; Gambarotta, S. *Organometallics* **1994**, *13*, 1326.

(5) Noh, S.-K.; Heintz, R. A.; Theopold, K. H. *Organometallics* **1989**, *8*, 2071.
 (6) Bhandari, G.; Kim, Y.; McFarland, J. M.; Rheingold, A. L.; Theopold, K. H. *Organometallics* **1995**, *14*, 738.
 (7) Heintz, R. A.; Leelasubcharoen, S.; Liable-Sands, L. M.; Rheingold, A. L.; Theopold, K. H. *Organometallics* **1998**, *17*, 5477.
 (8) Noh, S.-K.; Heintz, R. A.; Janiak, C.; Sendlinger, S. C.; Theopold, K. H. *Angew. Chem., Int. Ed. Engl.* **1990**, *29*, 775.
 (9) Theopold, K. H. *Acc. Chem. Res.* **1990**, *23*, 263.
 (10) Hessen, B.; Meetsma, A.; Teuben, J. H. *J. Am. Chem. Soc.* **1989**, *111*, 5977.

Scheme 1

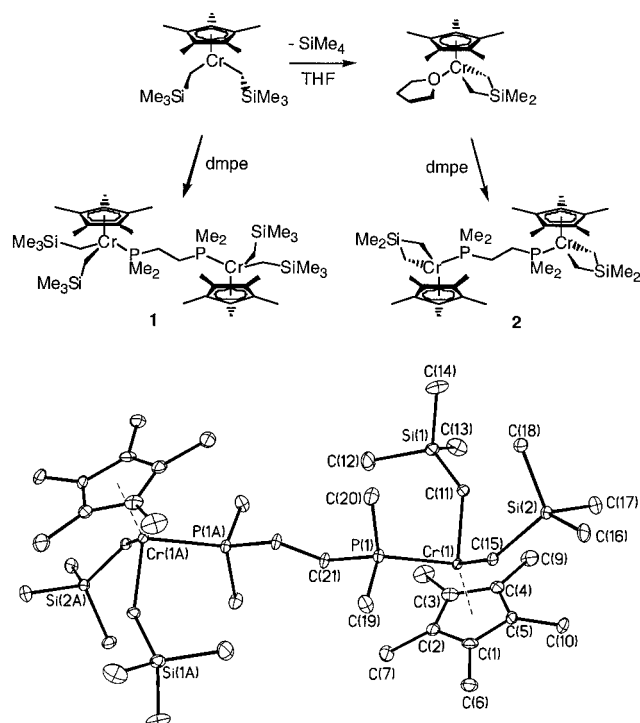


Figure 1. Molecular structure of $[\text{Cp}^*\text{Cr}(\text{CH}_2\text{SiMe}_3)_2]_2(\mu\text{-}\eta^1\text{:}\eta^1\text{-dmpe})$ (**1**, thermal ellipsoids are shown at 30% probability). Selected interatomic distances and angles are listed in Table 1.

Table 1. Selected Interatomic Distances and Angles for $[\text{Cp}^*\text{Cr}(\text{CH}_2\text{SiMe}_3)_2]_2(\mu\text{-}\eta^1\text{:}\eta^1\text{-dmpe})$ (1**)**

Distances (Å)			
Cr(1)–P(1)	2.4465(6)	Cr(1)–C(11)	2.123(2)
Cr(1)–C(15)	2.144(2)	Cr(1)–C(1)	2.309(2)
Cr(1)–C(2)	2.334(2)	Cr(1)–C(3)	2.296(2)
Cr(1)–C(4)	2.268(2)	Cr(1)–C(5)	2.288(2)
C(11)–Si(1)	1.861(2)	C(15)–Si(2)	1.869(2)
Cr(1)–cent ^a	1.955(2)		
Angles (deg)			
P(1)–Cr(1)–C(11)	94.05(7)	P(1)–Cr(1)–C(15)	87.42(6)
C(11)–Cr(1)–C(15)	95.57(9)	P(1)–Cr(1)–cent ^a	124.7(9)
C(11)–Cr(1)–cent ^a	125.0(9)	C(15)–Cr(1)–cent ^a	120.7(9)
Cr(1)–C(11)–Si(1)	138.44(13)	Cr(1)–C(15)–Si(2)	126.32(12)
Cr(1)–P(1)–C(21)			

^a cent is the centroid of the Cp* ligand.

The molecular structure of **1** has been determined by X-ray diffraction; the result is depicted in Figure 1, and selected interatomic distances and angles are listed in Table 1. The metric parameters are very similar to those of analogous compounds and merit no particular discussion. **1** finds close precedent in $[\text{CpCr}(\text{CH}_3)_2]_2(\mu\text{-}\eta^1\text{:}\eta^1\text{-dmpe})$, which was prepared by Poli et al. in an unsuccessful attempt to force CpCr^{III} to adopt a 17-electron configuration (i.e., $\text{Cp}(\text{dmpe})\text{CrMe}_2$).¹¹ The effective magnetic moment of **1** at room temperature measured $\mu_{\text{eff}} = 5.6(1)\mu_{\text{B}}$ ($3.9\mu_{\text{B}}$ per Cr), consistent with the absence of any magnetic interaction mediated by the bridging diphosphine ligand.

The formation of **1** suggested that alkane elimination should precede the addition of the chelating ligand. In that vein we note that the dissolution of metallacyclobu-

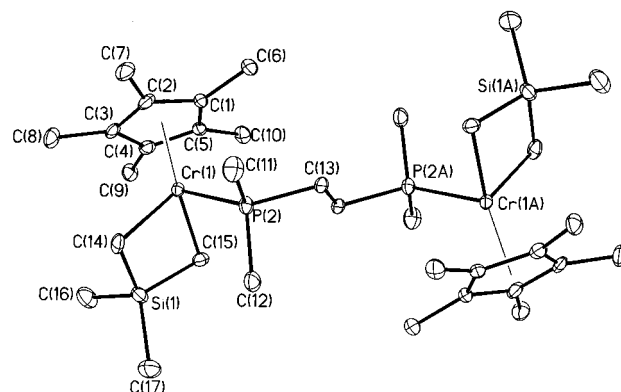


Figure 2. Molecular structure of $[\text{Cp}^*\text{Cr}(\text{CH}_2)_2\text{SiMe}_2]_2(\mu\text{-}\eta^1\text{:}\eta^1\text{-dmpe})$ (**2**, thermal ellipsoids are shown at 30% probability). Selected interatomic distances and angles are listed in Table 2.

Table 2. Selected Interatomic Distances and Angles for $[\text{Cp}^*\text{Cr}(\text{CH}_2)_2\text{SiMe}_2]_2(\mu\text{-}\eta^1\text{:}\eta^1\text{-dmpe})$ (2**)**

Distances (Å)			
Cr(1)–P(2)	2.4292(16)	Cr(1)–C(14)	2.113(6)
Cr(1)–C(15)	2.107(6)	Cr(1)–C(1)	2.281(5)
Cr(1)–C(2)	2.271(5)	Cr(1)–C(3)	2.276(5)
Cr(1)–C(4)	2.271(6)	Cr(1)–C(5)	2.279(5)
C(14)–Si(1)	1.860(6)	C(15)–Si(2)	1.851(6)
Cr(1)–cent ^a	1.929(5)		
Angles (deg)			
P(2)–Cr(1)–C(14)	89.86(17)	P(2)–Cr(1)–C(15)	92.84(17)
C(14)–Cr(1)–C(15)	83.6(2)	P(2)–Cr(1)–cent ^a	126.9(15)
C(14)–Cr(1)–cent ^a	125.6(15)	C(15)–Cr(1)–cent ^a	125.5(15)
Cr(1)–C(14)–Si(1)	87.8(2)	Cr(1)–C(15)–Si(2)	88.2(2)
Cr(1)–P(2)–C(13)	118.15(18)	C(14)–Si(1)–C(15)	98.6(3)

^a cent is the centroid of the Cp* ligand.

tane $\text{Cp}^*(\text{THF})\text{Cr}(\text{CH}_2)_2\text{SiMe}_2$ in pentane had yielded the bis(μ -alkylidene) complex $[\text{Cp}^*\text{Cr}(\mu\text{-CHSiMe}_3)]_2$, among the erstwhile observations pointing toward an interconversion between **A** and **B**. Consequently, addition of dmpe to $\text{Cp}^*(\text{THF})\text{Cr}(\text{CH}_2)_2\text{SiMe}_2$ was tried. This reaction yielded a green complex, to which we assign the structure $[\text{Cp}^*\text{Cr}(\text{CH}_2)_2\text{SiMe}_2]_2(\mu\text{-}\eta^1\text{:}\eta^1\text{-dmpe})$ (**2**, see Scheme 1). The molecular structure of **2** has been determined by X-ray diffraction; the molecule is shown in Figure 2, and selected interatomic distances and angles are listed in Table 2. Once again, a dinuclear complex held together by a bridging diphosphine was produced. It is possible that the ligand substitution reaction proceeds too fast to allow for rearrangement of the coordinatively unsaturated metallacycle (**B**) to the alkylidene species (**A**). However, another possible interpretation posits that the greater stability of the coordinatively saturated metallacycle is reflected in the transition state of the trapping step, effectively draining the equilibrating intermediate(s) into **2**. The magnetic behavior of **2** ($\mu_{\text{eff}} = 5.6(1)\mu_{\text{B}}$, i.e., $3.9\mu_{\text{B}}$ per Cr) again rules out any magnetic interaction between the metal atoms. An alternative method of preparation of **2** is the thermal decomposition of **1**; ¹H NMR monitoring of a solution of **1** heated to 60 °C showed the gradual appearance of the resonances of **2** and SiMe_4 .

The structures of **1** and **2** suggested that dmpe, albeit a potent bidentate ligand, is too flexible to serve our purpose. In other words, we need a bidentate ligand that by its very nature can coordinate to one metal only, thus leaving only a single coordination site on chromium for

(11) Fetting, J. C.; Mattamana, S. P.; Poli, R.; Rogers, R. D. *Organometallics* **1996**, *15*, 4211.

Scheme 2

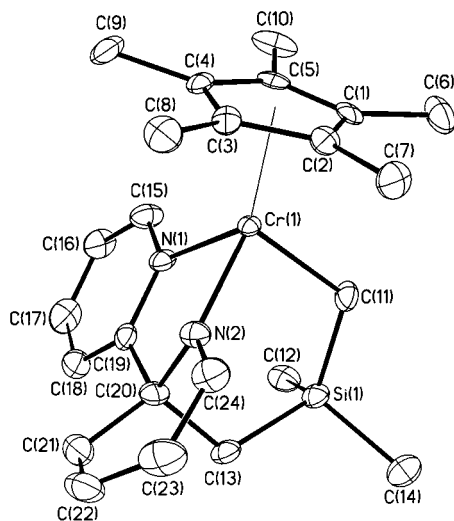
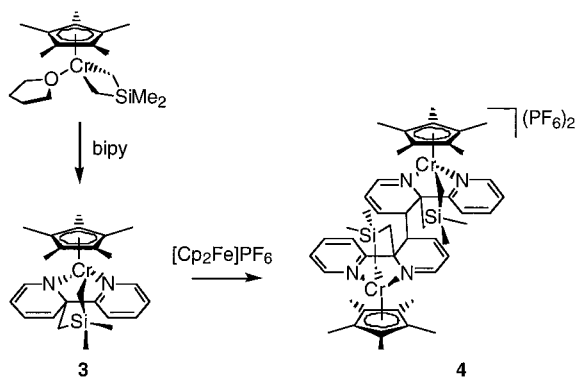


Figure 3. Molecular structure $\text{Cp}^*\text{Cr}(\eta^3\text{-C}_{14}\text{H}_{18}\text{N}_2\text{Si})$ (**3**, thermal ellipsoids are shown at 30% probability). Selected interatomic distances and angles are listed in Table 3.

binding of the alkyl-derived moiety. Such a ligand is 2,2'-bipyridine (bipy). We remind the reader that reaction of dialkyls $\text{Cp}^*(\text{L})\text{CrR}_2$ with bipy resulted in homolysis of a Cr–C bond and isolation of Cr^{II} alkyls of the type $\text{Cp}^*(\text{bipy})\text{CrR}$.⁶ However, trapping of an **A/B** mixture with bipy might reasonably be expected to favor the alkylidene isomer **A**. With this notion in mind, we investigated the reaction of $\text{Cp}^*(\text{THF})\text{Cr}(\text{CH}_2)_2\text{SiMe}_2$ with bipyridine.

Addition of 1 equiv of bipy to a THF solution of $\text{Cp}^*(\text{THF})\text{Cr}(\text{CH}_2)_2\text{SiMe}_2$ yielded a dark green solution. Standard workup and recrystallization from toluene/pentane yielded a new chromium complex (**3**, see Scheme 2) that appeared to contain a bipy ligand as well as a silicon-containing organic ligand. As the spectroscopic data were not sufficient to assign a structure to the newly formed compound, a crystal structure determination was necessary to ascertain its identity. The molecular structure of **3** is shown in Figure 3, and selected interatomic distances and angles are listed in Table 3. As anticipated, the product is a mononuclear complex, but instead of the hoped for alkylidene, **3** contains a functionalized bipy ligand. Specifically, one of the termini of the metallacycle has been transferred from chromium to the 2-position of the bipyridine, forming a new C–C bond and thereby creating a quaternary carbon as well as transforming the adjacent nitrogen from a neutral two-electron donor into an

Table 3. Selected Interatomic Distances and Angles for $\text{Cp}^*\text{Cr}(\eta^3\text{-C}_{14}\text{H}_{18}\text{N}_2\text{Si})$ (**3**)

Distances (Å)			
Cr(1)–N(1)	2.056(4)	Cr(1)–N(2)	1.981(4)
Cr(1)–C(11)	2.098(5)	Cr(1)–C(1)	2.264(5)
Cr(1)–C(2)	2.247(5)	Cr(1)–C(3)	2.290(5)
Cr(1)–C(4)	2.295(5)	Cr(1)–C(5)	2.284(5)
Cr(1)–cent ^a	1.933(5)	C(11)–Si(1)	1.828(6)
Si(1)–C(13)	1.903(5)	C(13)–C(20)	1.565(7)
C(19)–C(20)	1.522(7)	N(2)–C(20)	1.485(7)
C(20)–C(21)	1.500(7)	C(21)–C(22)	1.342(9)
C(22)–C(23)	1.453(10)	C(23)–C(24)	1.369(8)
C(24)–N(2)	1.358(7)		
Angles (deg)			
N(1)–Cr(1)–N(2)	79.90(16)	N(1)–Cr(1)–C(11)	92.87(18)
N(2)–Cr(1)–C(11)	92.62(19)	N(1)–Cr(1)–cent ^a	129.4(19)
N(2)–Cr(1)–cent ^a	129.5(19)	C(11)–Cr(1)–cent ^a	120.3(19)
Cr(1)–C(11)–Si(1)	117.5(2)	C(11)–Si(1)–C(13)	111.1(2)
Si(1)–C(13)–C(20)	116.5(3)	Cr(1)–N(1)–C(15)	125.8(3)
Cr(1)–N(1)–C(19)	115.3(3)	C(15)–N(1)–C(19)	118.8(4)
Cr(1)–N(2)–C(20)	115.0(3)	Cr(1)–N(2)–C(24)	128.6(4)
C(20)–N(2)–C(24)	114.1(4)		

^a cent is the centroid of the Cp^* ligand.

amido ligand. The coordination environment of the chromium thus comprises one alkyl, one amide, and one neutral pyridine donor ligand besides the Cp^* ligand. The formal oxidation state of chromium remains +III, and the magnetic moment of **3** ($\mu_{\text{eff}} = 3.6(1)\mu_{\text{B}}$) is consistent with that assignment. It is notable that this rearrangement breaks the aromaticity of one of the two linked pyridine moieties. Indeed, careful inspection of the bond distances in this newly formed nitrogen heterocycle reveals pronounced bond length alternation. Thus N(2)–C(20) (1.49 Å) and C(20)–C(21) (1.50 Å) are clearly single bonds to the new quaternary carbon atom (C(20)). The next four contiguous bonds in the ring (i.e., C(21)–C(22), 1.34 Å; C(22)–C(23), 1.45 Å; C(23)–C(24), 1.37 Å; and C(24)–N(2), 1.36 Å) show a pattern of bond distances that is typical for 1,2-dihydropyridines, even though the C(24)–N(2) distance may seem rather short for a formal single bond. Molecular mechanics or semiempirical quantum calculations (e.g., PM3) on the free ligand give distances that are very close to the observed ones;¹² moreover, the relevant distances in the crystal structure of an authentic 1,2-dihydropyridine derivative are all but indistinguishable from those of **3**.¹³ The Cr–N(2) distance of 1.98 Å is shorter than the characteristic Cr–N distance for chromium bipyridine complexes (2.08 Å) and supports the interpretation as a Cr–amide bond. All these structural observations are consistent with a reduction of the pyridine moiety to the deprotonated form of a 1,2-dihydropyridine derivative. The metric parameters of the other pyridine ring do not deviate from those expected of a bipyridine ligand.

The mechanism of formation of **3** is somewhat ambiguous. Dissociative ligand substitution of THF by bipy apparently yields the metallacycle $\text{Cp}^*(\eta^2\text{-bipy})\text{Cr}(\text{CH}_2)_2\text{-SiMe}_2$. Such pseudo seven-coordinate $\text{Cp}^*\text{Cr}^{\text{III}}$ species are essentially unknown and likely to be highly destabilized.^{9,14} One possible follow-up reaction involves a migratory insertion of a N–C multiple bond of coordi-

(12) The calculations were performed with CS Chem3D Pro, Version 5.0; CambridgeSoft, 1999.

(13) Kozhushkov, S. I.; Brandl, M.; Yufit, D. S.; Machinek, R.; Demeijere, A. *Liebigs Ann.-Recl.* **1997**, 2197–2204.

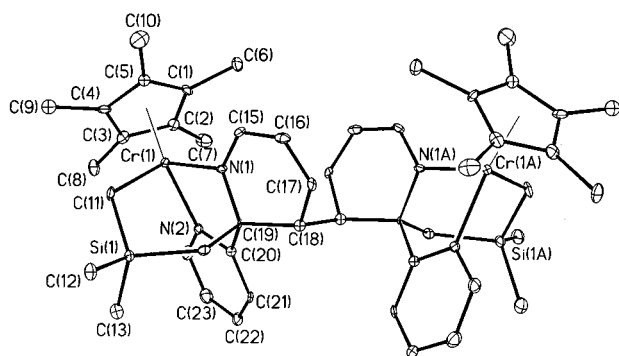


Figure 4. Molecular structure of $[\text{Cp}^*\text{Cr}(\mu\text{-}\eta^3\text{:}\eta^3\text{-C}_{28}\text{H}_{36}\text{N}_4\text{-Si}_2)](\text{PF}_6)_2$ (**4**)· $2\text{CH}_2\text{Cl}_2$; only the dicationic chromium complex is shown (thermal ellipsoids are shown at 30% probability). Selected interatomic distances and angles are listed in Table 4.

nated bipy into either Cr–C bond of the metallacycle, thereby forming **3** directly. The previously observed insertion of nitriles into $\text{Cp}^*\text{Cr}^{\text{III}}$ -alkyls provides some precedent for this pathway. However, based on the reactions of acyclic chromium dialkyls with bipy (see above), we consider a homolytic cleavage of one Cr–C bond, followed by attack of the tethered alkyl radical on the bipy ligand, to be the more probable course of reaction. Either way, we are not aware of any previous report of this kind of attack on a coordinated bipyridine ligand. The loss of aromaticity of a pyridine ring (estimated at 130 kJ/mol) provides yet another measure of the reluctance of Cr^{III} to support a terminal alkylidene.

We believe that the apparent instability of the target molecule is due to an unfavorable electronic interaction. The filled p-orbital of the alkylidene dianion (here CHSiMe_3^{2-}) overlaps with a d-orbital of π -symmetry on chromium; however, for Cr^{III} (d^3) the latter is actually occupied by one electron; that is, this is a two-center/three-electron interaction. The antibonding orbital of the Cr–C π -bond bond is half-filled and the bond is weak. It appears that the π -donation from the alkylidene is not strong enough to enforce spin pairing to a doublet state. In essence, the pairing energy of Cr^{III} wins out over the chance to form a chromium–carbon π -bond. If this is true, removal of the offending electron, e.g., by oxidation of the complex to Cr^{IV} (d^2), might stabilize the desired alkylidene. With this rationale in mind we have investigated the products of the chemical oxidation of **3**, in the hope that the rearrangement would prove reversible.

Reaction of **3** with 1 equiv of $[\text{Cp}_2\text{Fe}]\text{PF}_6$ was fast and yielded ferrocene and a new chromium complex, **4** (see Scheme 2). Judging from its solubility characteristics and IR spectrum, **4** was a hexafluorophosphate salt. Its paramagnetism made a characterization by NMR spectroscopy impractical; hence the crystal structure of **4** was determined by X-ray diffraction. The result is depicted in Figure 4, and selected interatomic distances and angles are listed in Table 4. Obviously, **4** is not the desired $[\text{Cp}^*(\text{bipy})\text{Cr}(\text{CHSiMe}_3)]\text{PF}_6$ but rather a dimer of the one-electron oxidation product 3^+ . A 2-fold

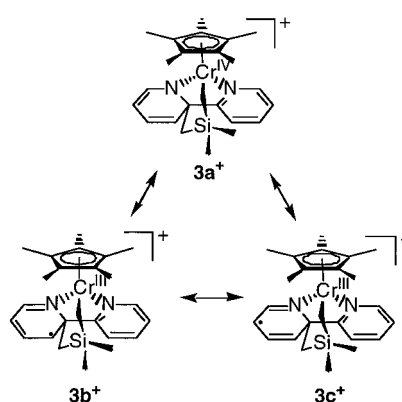
Table 4. Selected Interatomic Distances and Angles for $[\text{Cp}^*\text{Cr}(\mu\text{-}\eta^3\text{:}\eta^3\text{-C}_{28}\text{H}_{36}\text{N}_4\text{Si}_2)](\text{PF}_6)_2$ (**4**)· $2\text{CH}_2\text{Cl}_2$

Distances (Å)			
Cr(1)–N(1)	2.031(5)	Cr(1)–N(2)	2.070(5)
Cr(1)–C(11)	2.069(7)	Cr(1)–C(1)	2.258(7)
Cr(1)–C(2)	2.257(7)	Cr(1)–C(3)	2.226(7)
Cr(1)–C(4)	2.248(7)	Cr(1)–C(5)	2.244(7)
Cr(1)–cent ^a	1.894(6)	C(11)–Si(1)	1.848(7)
Si(1)–C(14)	1.901(6)	C(14)–C(19)	1.546(9)
C(19)–C(20)	1.511(9)	N(1)–C(15)	1.278(9)
C(15)–C(16)	1.446(10)	C(16)–C(17)	1.339(9)
C(17)–C(18)	1.499(9)	C(18)–C(19)	1.559(8)
C(19)–N(1)	1.489(8)	C(18)–C(18A)	1.608(13)

Angles (deg)			
N(1)–Cr(1)–N(2)	78.6(2)	N(1)–Cr(1)–C(11)	89.3(2)
N(2)–Cr(1)–C(11)	96.7(3)	N(1)–Cr(1)–cent ^a	131.0(5)
N(2)–Cr(1)–cent ^a	129.2(4)	C(11)–Cr(1)–cent ^a	119.6(5)
Cr(1)–C(11)–Si(1)	116.9(4)	C(11)–Si(1)–C(14)	108.3(3)
Si(1)–C(14)–C(19)	116.5(4)	Cr(1)–N(1)–C(15)	126.4(5)
Cr(1)–N(1)–C(19)	114.4(4)	C(15)–N(1)–C(19)	118.8(5)
Cr(1)–N(2)–C(20)	116.5(4)	Cr(1)–N(2)–C(24)	125.2(5)
C(20)–N(2)–C(24)	118.1(6)		

^a cent is the centroid of the Cp^* ligand.

Scheme 3



rotational axis renders only half of the molecule unique. The basic structure of **3** remains intact, but a new, long carbon–carbon bond (1.61 Å) couples the original bipy ligands of two such units at their 3-positions. This further elaboration transforms the 1,2-dihydropyridine anion of **3** into a neutral 2,3-dihydropyridine derivative. The bond distances in this ring and the longer Cr–N distance (Cr(1)–N(1), 2.03 Å) are consistent with this picture. Despite the removal of one electron per metal atom, the chromium retains its formal oxidation state of +III; the ligand has been oxidized instead. The magnetic moment of **4** ($\mu_{\text{eff}} = 5.4(1)\mu_{\text{B}}$, i.e., $3.8\mu_{\text{B}}/\text{Cr}$) is consistent with magnetically dilute Cr^{III} ions. In this context, and as an explanation for the formation of **4**, it is instructive to consider the possible resonance forms of the initial oxidation product 3^+ (see Scheme 3). Structure **3a**⁺ with its tetravalent chromium is probably the most important contributor. However, delocalization of the hole in the trio of SOMOs onto the unsaturated ligand (or in other words charge transfer from the amide to the metal) results in structures **3b**⁺ and **3c**⁺, with radical character in the 3- or 5-position of the ring. Coupling of two such radicals allows chromium to return to its favored oxidation state of +III. The conjugated double bonds of **3b**⁺ probably render it slightly more stable, hence the formation of the 3,3-coupled isomer **4** as the final product.

(14) For the ESR spectroscopic detection of a minute equilibrium concentration of presumed $[\text{Cp}^*\text{Cr}(\text{CN})_4]^{2-}$ see: Mattamana, S. P.; Poli, R. *Organometallics* **1997**, *16*, 2427.

We note that the oxidative transformation of **3** into **4** does not necessarily invalidate our line of reasoning concerning the stabilization of a chromium alkylidene. The C–C bond formation leading to **3** may be irreversible, at least on the time scale of the oxidation and subsequent dimerization ($k_{\text{dim}} = 2 \times 10^4 \text{ M}^{-1} \text{ s}^{-1}$) of the latter.¹⁵

Conclusions

Once again we have tried, and failed, to isolate a terminal alkylidene bonded to the $\text{Cp}^*\text{Cr}^{\text{III}}$ fragment. The varied escape routes by which chromium avoids the formation of such a species bespeak its fundamental instability. In the case described herein it leads to the loss of aromatic stabilization of half of a bipyridine ligand. Higher oxidation states of chromium may be needed to support a chromium–carbon double bond. However, oxidation of rearrangement product **3** did not reverse the functionalization of the bipyridine ligand. Rather, further ligand coupling ensued. These results reemphasize the notion that any terminal $\text{Cp}^*\text{Cr}^{\text{III}}$ alkylidene will be destabilized and therefore highly reactive.

Experimental Section

General Considerations. All manipulations of compounds were performed using standard Schlenk, high-vacuum, and inert atmosphere glovebox techniques. Pentane, diethyl ether, tetrahydrofuran (THF), and toluene were distilled from purple Na benzophenone/ketyl solutions. C₆D₆ was predried with Na and stored under vacuum over Na/K alloy. CH₂Cl₂ and CD₂-Cl₂ were predried with CaH₂ and stored under vacuum over 4 Å molecular sieves. CrCl₃(anhydrous) was purchased from Strem Chemical Co. Trimethylsilylmethylolithium, dmpe, bipy, and [Cp₂Fe]PF₆ were purchased from Aldrich Chemical Co. CrCl₃(THF)₃,¹⁶ Cp*Li,¹⁷ Cp*Cr(CH₂SiMe₃)₂,⁷ and Cp*(THF)-Cr(CH₂)₂SiMe₃⁷ were synthesized by literature procedures.

NMR spectra were recorded on Bruker AM-250, WM-250, or DRX-400 spectrometers and were referenced to the residual protons of the solvent ($\text{C}_6\text{D}_5\text{H}$, 7.15 ppm; CDCl_2 , 5.32 ppm). FTIR spectra were recorded on a Mattson Alpha Centauri spectrometer. UV-visible spectra were obtained with a Hewlett-Packard HP845x spectrometer. Mass spectral analyses were performed by the University of Delaware Mass Spectrometry Facility. Elemental analyses were obtained from Schwarzkopf Microanalytical Laboratory, Inc., Woodside, NY 11377. Room-temperature magnetic susceptibilities were determined using a Johnson Matthey magnetic susceptibility balance, which utilizes a modification of the Gouy method. Molar magnetic susceptibilities were corrected for diamagnetism using Pascal constants.

Synthesis of [Cp*Cr(CH₂SiMe₃)₂]₂(μ-η¹:η¹-dmpe) (1). A 460 μL (2.757 mmol) portion of dmpe was slowly injected into a stirred red solution of 1 g (2.765 mmol) of Cp*Cr(CH₂SiMe₃)₂ in 10 mL of pentane. The color of the solution immediately changed to blue-green. After the mixture was stirred for 1 h, the solution was concentrated and crystallized at -30 °C to yield 1.160 g of blue-purple solid **1** (96% yield). ¹H NMR (C₆D₆): -18.31 (br, 6H), -0.77 (br, 18H), 5.55 (br, 15H) ppm. IR (KBr): 2940 (s), 2893 (s), 2827 (s), 1486 (w), 1421 (s), 1375 (m), 1390 (m), 1282 (m), 1233 (s), 1187 (m), 1175 (w), 927 (s), 897 (s), 852 (s), 821 (s), 721 (s), 671 (s), 516 (w), 424 (w) cm⁻¹.

UV/vis (pentane): 354 ($\epsilon = 10254 \text{ M}^{-1} \text{ cm}^{-1}$), 488 ($\epsilon = 1472 \text{ M}^{-1} \text{ cm}^{-1}$) nm. Mp: 131–133 °C (dec). μ_{eff} (295 K) = $5.6(1)\mu_{\text{B}}$. Anal. Calcd for $\text{C}_{42}\text{H}_{90}\text{Cr}_2\text{Si}_4\text{P}_2$: C, 57.75; H, 10.39. Found: (1) C, 51.86; H, 9.22; (2) C, 55.89; H, 9.39.¹⁸ MS, *m/z*: 649 (6.9%), 606 (35.7%), 553 (49.2%), 422 (13.3%), 322 (100%).

Synthesis of $[\text{Cp}^*\text{Cr}((\text{CH}_2)_2\text{SiMe}_2)_2]_2[\mu\text{-}\eta^1\text{-}\eta^1\text{-dmpe}]$ (2**).** A 880 mg (2.433 mmol) portion of $\text{Cp}^*\text{Cr}(\text{CH}_2\text{SiMe}_3)_2$ was dissolved in 10 mL of THF, and the solution was heated to 50 °C for 18 h. To this dark green solution of $\text{Cp}^*(\text{THF})\text{Cr}(\text{CH}_2)_2\text{-SiMe}_2$ formed in situ was added 410 μL (2.458 mmol) of dmpe, and the solution was allowed to stir for 1 h. The THF and excess dmpe were removed by rotoevaporation to leave a green solid. This solid was dissolved in toluene, layered with pentane, and cooled to -30 °C to give 270 mg of **2** (32% yield). ^1H NMR (C_6D_6): -31.03 (br, 2H), -12.57 (br, 6H), 27.05 (br, 15H) ppm. IR (KBr): 2933 (s), 2907 (s), 1481 (w), 1420 (s), 1375 (m), 1283 (m), 1231 (s), 1089 (m), 942 (s), 922 (s), 831 (s), 775 (m), 720 (m), 677 (s), 486 (s) cm^{-1} . UV/vis (toluene): 408 ($\epsilon = 2797 \text{ M}^{-1} \text{ cm}^{-1}$), 625 ($\epsilon = 1805 \text{ M}^{-1} \text{ cm}^{-1}$) nm. $\mu_{\text{eff}}(295 \text{ K}) = 5.60 \mu_{\text{B}}$. Anal. Calcd for $\text{C}_{34}\text{H}_{66}\text{Cr}_2\text{Si}_2\text{P}_2$: C, 58.59; H, 9.54. Found: (1) C, 54.95; H, 8.94; (2) C, 54.41; H, 10.00.¹⁸ MS, m/e : 680 (90.7%), 649 (53.5%), 606 (72.6%), 546 (100%), 510 (20.1%), 476 (17.4%), 376 (11.1%).

Synthesis of (η^5 -Pentamethylcyclopentadienyl)(2-(2''-2'-dimethyl-2''-silapropyl)-1,2-dihydro[2,2']bipyridine-1,3''-diyl)chromium(III), $\text{Cp}^*\text{Cr}(\eta^3\text{-C}_{14}\text{H}_{18}\text{N}_2\text{Si})$ (3**).** A 1.54 mg (4.258 mmol) sample of $\text{Cp}^*\text{Cr}(\text{CH}_2\text{Si}(\text{CH}_3)_3)_2$ was dissolved in 10 mL of THF and then was heated at 50 °C for 18 h. To this dark green solution was added 665 mg (2.458 mmol) of bpy, and the solution was allowed to stir for 1 h. The THF was removed by rotoevaporation, leaving a green-black solid. This solid was dissolved in toluene and layered with pentane and cooled at -30 °C to give 582 mg of **3** (32% yield). ^1H NMR (C_6D_6): -80.71, -71.86, -6.01, 2.87, 17.11, 42.97, 54.64 ppm. IR (KBr): 2940 (s), 2855 (s), 1589 (m), 1486 (s), 1376 (m), 1256 (s), 1059 (w), 1024 (w), 976 (w), 895 (s), 833 (s), 790 (m), 726 (m), 676 (w) cm^{-1} . UV/vis (toluene): 374 ($\epsilon = 8368 \text{ M}^{-1} \text{ cm}^{-1}$), 579 ($\epsilon = 1902 \text{ M}^{-1} \text{ cm}^{-1}$) nm. Mp: 158 °C (dec). μ_{eff} (296 K) = 3.64 μ_{B} . Anal. Calcd for $\text{C}_{24}\text{H}_{33}\text{CrSiN}_2$: C, 67.01; H, 7.74; N, 6.52. Found: C, 66.82; H, 8.01; N, 6.59. MS, m/e : 429 (16.0%), 343 (100%), 295 (22.4%), 208 (19.6%).

Synthesis of $[\text{Cp}^*\text{Cr}(\mu\text{-}\eta^3\text{:}\eta^3\text{-C}_{28}\text{H}_{36}\text{N}_4\text{Si}_2)[\text{PF}_6]_2$ (4**).** **2CH₂Cl₂.** A 250 mg (0.756 mmol) sample of $[\text{Cp}_2\text{Fe}][\text{PF}_6]$ was added to a stirred green solution of 325 mg (0.756 mmol) of **3** in 25 mL of THF. After a few minutes, the color of the solution changed to brown-yellow. After the mixture was allowed to stir for a half an hour the solvent was removed by rotoevaporation, leaving a brown-black solid. This solid was washed with pentane and filtered, giving a yellow filtrate and a red-black solid. Pentane was evaporated from the filtrate to yield 130 mg of Cp_2Fe as a yellow solid (92%). The red-black solid was recrystallized from methylene chloride layered with pentane at -30°C , yielding 450 mg of **4**·2CH₂Cl₂ (90%). ^1H NMR ($\text{CD}_2\text{-Cl}_2$): $-\text{67.58}$, $-\text{19.69}$, 0.01 , 7.17 , 19.34 , 23.27 , 33.70 , 44.03 , 47.31 ppm. IR (KBr): 2918 (m), 1474 (m), 1431 (m), 842 (s), 737 (m), 557 (m). UV/vis (CH_2Cl_2): 378 ($\epsilon = 12613 \text{ M}^{-1} \text{ cm}^{-1}$), 463 ($\epsilon = 8570 \text{ M}^{-1} \text{ cm}^{-1}$) nm. Mp: $>280^\circ\text{C}$. $\mu_{\text{eff}}(297 \text{ K}) = 5.4(1)\mu_{\text{B}}$. Anal. Calcd for $\text{C}_{50}\text{H}_{70}\text{Cr}_2\text{Si}_2\text{N}_4\text{P}_2\text{F}_{12}\text{Cl}_4$: C, 45.53; H, 5.35; N, 4.25. Found: C, 45.74; H, 5.52; N, 4.22. MS, m/e (%): 343 (12%), 222 (5.3%), 170 (65.9%), 156 (64.8%), 119 (22.7%), 77 (100%).

(15) Leelasubcharoen, S.; Lehmann, M. W.; Theopold, K. H.; Evans, D. H. *J. Electrochem. Soc.*, in press.

(16) Herwig, W.; Zeiss, H. H. *J. Org. Chem.* **1958**, 23, 1404.

(17) Threlkel, R. S.; Bercaw, J. E.; Seidler, P. F.; Stryker, J. M.; Bergman, R. G. *Org. Synth.* **1987**, *65*, 42.

(18) Despite repeated attempts, triply recrystallized samples of **1** and **2** did not give satisfactory elemental analyses. **1** is thermally labile, and both **1** and **2** are very air-sensitive; we submit that decomposition during shipping or handling is the cause of this failure. ¹H NMR spectra of these complexes are included in the Supporting Information; however, the extreme broadening of the resonances due to the paramagnetism of the complexes renders this way of demonstrating purity ambiguous as well.

Table 5. Crystallographic Data for [Cp*Cr(CH₂SiMe₃)₂]₂(μ-η¹:η¹-dmpe) (1), [Cp*Cr(CH₂)₂SiMe₂]₂(μ-η¹:η¹-dmpe) (2), Cp*Cr(η³-C₁₄H₁₈N₂Si) (3), and [Cp*Cr(μ-η³:η³-C₂₈H₃₆N₄Si₂)] [PF₆]₂ (4)·2CH₂Cl₂

	1	2	3	4
formula	C ₄₂ H ₉₀ Cr ₂ P ₂ Si ₄	C ₃₄ H ₆₆ Cr ₂ P ₂ Si ₂	C ₂₄ H ₃₃ CrN ₂ Si	C ₅₀ H ₇₀ Cl ₄ Cr ₂ F ₁₂ N ₄ P ₂ Si ₂
fw	873.44	696.99	429.61	1319.02
space group	<i>P</i> 2 ₁ / <i>n</i>	<i>P</i> 2 ₁ / <i>n</i>	<i>P</i> 2 ₁ / <i>c</i>	<i>P</i> 2 ₁ 2 ₁ 2
<i>a</i> , Å	9.4135(2)	11.7706(2)	9.4575(2)	14.5689(2)
<i>b</i> , Å	19.5070(2)	11.4745(2)	16.8771(2)	18.6603(2)
<i>c</i> , Å	14.2857(2)	14.8858(3)	14.6778(2)	10.86420(10)
α, deg	90.00	90.00	90.00	90.00
β, deg	92.7572(6)	103.2229(12)	105.0810(10)	90.00
γ, deg	90.00	90.00	90.00	90.00
<i>V</i> , Å ³	2620.24(4)	1957.20(6)	2262.11(6)	2953.54(6)
<i>Z</i>	2	2	4	2
cryst color, habit	purple rod	green-blue plate	purple blade	brown plate
<i>D</i> (calc), g cm ⁻³	1.107	1.183	1.261	1.483
μ(Mo Kα), cm ⁻¹	5.92	7.19	5.70	7.20
temp, K	173(2)	173(2)	203(2)	173(2)
diffractometer radiation			Siemens P4/CCD Mo Kα (λ = 0.71073 Å)	
<i>R</i> (<i>F</i>), % ^a	4.42	6.65	6.93	7.26
<i>R</i> (<i>wF</i>), % ^a	14.68	18.13	16.20	21.27

^a Quantity minimized = $R(wF^2) = \sum [w(F_o^2 - F_c^2)^2] / \sum [(wF_o^2)^2]^{1/2}$; $R = \sum \Delta / \sum (F_o)$, $\Delta = |F_o - F_c|$. $w = 1/[\sigma^2(F_o^2) + (aP)^2 + bP]$, $P = [2F_c^2 + \text{Max}(F_o, 0)]/3$.

Crystallographic Structure Determinations. Crystal, data collection, and refinement parameters are given in Table 5. The systematic absences in the diffraction data of all structures are uniquely consistent with the reported space groups. The structures were solved using direct methods, completed by subsequent difference Fourier syntheses and refined by full-matrix least-squares procedures. The asymmetric units of **1** and **2** contain half of the dimers, which both lie on an inversion center. The asymmetric unit of **4** also contains half of the dimer, which lies on a 2-fold axis, as well as a PF₆ counterion and a dichloromethane molecule. No absorption correction was applied to the data of **1** and **3**, whereas SADABS absorption corrections were applied to the data of **2** and **4**. All non-hydrogen atoms were refined with anisotropic displacement coefficients, and hydrogen atoms were treated as idealized contributions.

All software and sources of scattering factors are contained in the SHELXTL (5.10) program library (G. Sheldrick, Siemens XRD, Madison, WI).

Acknowledgment. This research was supported by a grant from the National Science Foundation (CHE-9876426). S.L. thanks the Ministry of Science, Technology and Environment of Thailand for financial support.

Supporting Information Available: ¹H NMR spectra of **1** and **2**, and tables of crystal data, structure solution and refinement, atomic coordinates, interatomic distances and angles, anisotropic thermal parameters, and H-atom coordinates for **1**, **2**, **3**, and **4**. An X-ray crystallographic file, in CIF format, is available through the Internet only. This material is available free of charge via the Internet at <http://pubs.acs.org>.

OM0007421